Radar Cross Section Estimation of Open-Ended Cavities Using Physical Optics with Modified Vectors for Exterior and Iteration for Interior Walls

Ryosuke HASABA [1], Masakazu HARA[2], Makoto ANDO [1]

[1] Dept. of Electrical and Electronic Engineering, Tokyo Institute of Technology
2-12-1-S3-19, Ookayama, Meguro-ku, Tokyo, 152-8552, JAPAN
hasaba@antenna.ee.titech.ac.jp

[2]IHI Corporation, Toyosu IHI Building, 3-1-1, Toyosu, Koto-ku, Tokyo, 135-8710, JAPAN

Abstract

In this paper, we analyze electrical fields reflected from concave surface scatterers by independently applying the Iterative Physical Optics (IPO) for interior region and Modified Vector Physical Optics (MPO) for exterior region. Radar cross section (RCS) is given by the radiation integral over a closed surface consisting of complementary aperture and the conducting surfaces. The high accuracy of the method is demonstrated for the RCS of an open-ended cube.

Keywords : Modified-Vector Physical Optics Iterative Physical Optics Radar Cross Section Multiple Reflections

1. Introduction

Diffraction analyses for electromagnetic waves are generally reduced to the problems to derive secondary sources on the scatterers or the alternative equivalent surface. In low frequency, it's well known that various finite diference methods such as the Method of Moment (MoM), FEM and FDTD are effective and has high accuracy. However, in high frequency, the size of matrix is so large that we have difficulties in obtaining the current distributions. On the other hand, when we deal with high frequency problems, we can rely upon the locality of the scattering phenomena. Many HF diffraction techniques such as Geometrical Theory of Diffraction (GTD), Uniform Theory of Diffraction (UTD) and Physical Theory of Diffraction (PTD) utilize these assumptions a priori. Physical Optics (PO) also adopts implicitly this concept in defining the currents.

The Physical Optics (PO) is used widely because integration procedure remedies most of difficulties of HF techniques such as singularities and discontinuities in the fields, provided the computational load of integration is acceptable. For the accuracy enhancement of PO as the external problem, we have proposed to geometrically modify the definition of normal vector in PO, which is named as "Modified PO (MPO)". [1]-[2] On the other hand, multiple reflection in the internal problem, has been handled by the iterative use of PO [3],[4].

This paper discusses the RCS estimation of open-ended cavities or oversized cavities with multiple reflection, which has been computed by various analytical and asymptotic methods but has still been challenging. We calculate RCS by consistent use of PO for both interior and exterior regions, which is powered up by the above refinements. The Iterative Physical Optics and Modified-Vector Physical Optics are conducted independently in repective regions, on the assumption of locality; they are merged in a hybrid method in the final step of radiation integrals. The proposed method is applied for the open ended rectangular cavity or open-ended cavities and the comparison with MoM shows its reasonable accuracy.

2. Summary of Approaches

2.1 HYBRID METHOD

The induced currents on the inner walls of the cavity and those on the external walls are independently determined by using IPO and by using MPO respectively, as shown in Fig.1(a). The former provides the equivalent aperture fields over the cavity and the fields outside are given by the radiation integral over the closed surface consisting of the complementary area, that is the aperture and the conductor.

2.2 IPO METHOD

The Iterative Physical Optics is the method to represent multiple reflections.

By equivalent theorem, we compute electric and magnetic equivalent currents induced by incident EM field over the aperture as shown in Fig.(2-a).

$$\begin{cases} \boldsymbol{J}^i(\boldsymbol{r}'_a) = \hat{\boldsymbol{n}}' \times \boldsymbol{H}^i(\boldsymbol{r}'_a) \\ \boldsymbol{M}^i(\boldsymbol{r}'_a) = \boldsymbol{E}^i(\boldsymbol{r}'_a) \times \hat{\boldsymbol{n}}' \end{cases} \quad (1)$$

$\boldsymbol{E}^i$ and $\boldsymbol{H}^i$ are respectively incident electric field and magnetic field, $\boldsymbol{J}^i$ and $\boldsymbol{M}^i$ are respectively incident electric and magnetic equivalent currents induced over the aperture, $\boldsymbol{r}'_a$ is a point over the aperture , and $\hat{\boldsymbol{n}}'$ is the unit vector normal to the aperture.

We compute EM fields radiated by equivalent currents over the aperture on the inner walls of the cavity as shown in Fig.(2-a).

$$\boldsymbol{H}_c^i(\boldsymbol{r}_c) \approx \iint_{Sa} \boldsymbol{J}^i(\boldsymbol{r}'_a) \times \nabla G_0(\boldsymbol{r}_c - \boldsymbol{r}'_a)\, dSa' + \frac{1}{jkZ_0} \nabla \times \iint_{Sa} \boldsymbol{M}^i(\boldsymbol{r}'_a) \times \nabla G_0(\boldsymbol{r}_c - \boldsymbol{r}'_a)\, dSa' \quad (2)$$

The IPO method gives an initial value of

$$\boldsymbol{J}_0(\boldsymbol{r}_c) = \begin{cases} 2\hat{\boldsymbol{n}} \times \boldsymbol{H}_c^i(\boldsymbol{r}_c) & \text{Lit region} \\ 0 & \text{Shadow region} \end{cases} \quad (3)$$

which is by definition the PO currents on the wall excited by the incident sources in the aperture. $\boldsymbol{H}_c^i$ is the magnetic field on the inner wall of the cavity, ∇G_0 is the gradient of the free space Green's function, k is free space wave number, Z_0 is free space impedance, $\boldsymbol{r}_c$ is a point on the inner wall.

Iterative computation of currents induced on each facet of the inner walls of the cavity, due to the multiple reflections on the other facets of the inner walls as shown in Fig.(2-b).

$$\boldsymbol{J}_N(\boldsymbol{r}_c) = 2\hat{\boldsymbol{n}} \times \boldsymbol{H}_a^i(\boldsymbol{r}_c) + 2\hat{\boldsymbol{n}} \times \iint_{Sc} \boldsymbol{J}_{N-1}(\boldsymbol{r}'_c) \times \nabla G_0(\boldsymbol{r}_c - \boldsymbol{r}')\, dS'_c \quad (4)$$

$\boldsymbol{J}_N$ is the currents when this process is repeated N times until a stable value.

We compute currents induced on the aperture of EM fields scattered by the cavity inner walls as shown in Fig.(2-c).

$$\begin{cases} \boldsymbol{E}_{cav}^s(\boldsymbol{r}_a) \approx \dfrac{1}{jkY_0} \nabla \times \iint_{Sc} \boldsymbol{J}_N(\boldsymbol{r}'_c) \times \nabla G_0(\boldsymbol{r}_a - \boldsymbol{r}'_c)\, dSc' \\ \boldsymbol{H}_{cav}^s(\boldsymbol{r}_a) \approx \iint_{Sc} \boldsymbol{J}_N(\boldsymbol{r}'_c) \times \nabla G_0(\boldsymbol{r}_a - \boldsymbol{r}'_c)\, dSc' \end{cases} \quad (5)$$

We compute EM fields scattered at the observation point as shown in Fig.(2-d).

$$\begin{cases} \boldsymbol{J}^s(\boldsymbol{r}'_a) = (-\hat{\boldsymbol{n}}') \times \boldsymbol{H}_{cav}^s(\boldsymbol{r}'_a) \\ \boldsymbol{M}^s(\boldsymbol{r}'_a) = \boldsymbol{E}_{cav}^s(\boldsymbol{r}'_a) \times (-\hat{\boldsymbol{n}}') \end{cases} \quad (6)$$

$$\begin{cases} \boldsymbol{J}^{total}(\boldsymbol{r}'_a) = \boldsymbol{J}^s + \boldsymbol{J}^i \\ \boldsymbol{M}^{total}(\boldsymbol{r}'_a) = \boldsymbol{M}^s + \boldsymbol{M}^i \end{cases} \quad (7)$$

$$\boldsymbol{E}_{cav}^s(\boldsymbol{r}) = jk\eta \frac{e^{-jkr}}{4\pi r} \left(\iint_S \boldsymbol{J}^s e^{jk\hat{\boldsymbol{r}}\cdot\boldsymbol{q}} dS \times \hat{\boldsymbol{r}} \times \hat{\boldsymbol{r}} + \frac{1}{\eta} \iint_S \boldsymbol{M}^s e^{jk\hat{\boldsymbol{r}}\cdot\boldsymbol{q}} dS \times \hat{\boldsymbol{r}} \right) \quad (8)$$

2.3 THE MPO METHOD

PO defines induced currents on the illuminated region of the scattering surface by $\boldsymbol{I}_{PO} = 2\hat{\boldsymbol{n}} \times \boldsymbol{H}^i$, where vector $\hat{\boldsymbol{n}}$ is the unitary normal vector to the surface and $\boldsymbol{H}^i$ is the unperturbed incident field on the surface. The radiated fields are calculated by the surface integral of the PO currents based upon the field equivalent theorem, the PO currents $\boldsymbol{I}_{PO} = 2\hat{\boldsymbol{n}} \times \boldsymbol{H}^i$ are divided into two parts such as reflection components produced by a set of currents $\{\hat{\boldsymbol{n}} \times \boldsymbol{H}^i, -\boldsymbol{E}^i \times \hat{\boldsymbol{n}}\}$ and shadow components by $\{\hat{\boldsymbol{n}} \times \boldsymbol{H}^i, \boldsymbol{E}^i \times \hat{\boldsymbol{n}}\}$.

In MPO, the modified surface-normal vectors $\hat{\boldsymbol{n}}_r$ and $\hat{\boldsymbol{n}}_i$ are introduced as follows:

where $\boldsymbol{k}_d$ indicates the observer direction from the integration point on the scatterer, while the vectors $\boldsymbol{k}_i$ and $\boldsymbol{k}_{im}$ are the propagation vectors indicating the incident direction from the source and its (mirror) image, respectively and reflection region is above scatterer and the shadow region is the region underneath in the case that the source locates above scatterer as shown in Fig.3. The modified vector $\hat{n}_r$ is given by the reflection law between the observer and the source, while the vector $\hat{n}_i$ is similarly defined between the observer and an image source on the point of interest

$$\hat{n}_r = \pm\frac{\boldsymbol{k}_o - \boldsymbol{k}_i}{|\boldsymbol{k}_o - \boldsymbol{k}_i|}\quad\begin{pmatrix}+\text{: reflection region}\\ \pm\text{: shadow region}\end{pmatrix}\qquad \hat{n}_i = \mp\frac{\boldsymbol{k}_o - \boldsymbol{k}_{im}}{|\boldsymbol{k}_o - \boldsymbol{k}_{im}|}\quad\begin{pmatrix}+\text{: shadow region}\\ \mp\text{: reflection region}\end{pmatrix}\qquad (9)$$

4. Numerical Results

We use AFIM for currents over the aperture in order to confirm the effectiveness of IPO. The reference solutions were obtained using EM simulator and using AFIM. Fig. (4-a) and Fig. (4-b) shows the Electric Field of a rectangular cavity on the aperture with a length of 100 mm, a high of 100 mm and a width of 100 mm. The Electric field has been computed with the IPO method at 10 GHz, for an angle 30 degree with a VV polarization. IPO(0) is the case of no iterations, where the wall current is simply the first order PO currents. As N increases, the results improve at wider angles because more internal reflections are being included.

We have implemented the hybrid IPO/MPO method for 3D problem. Below we study the performance of this hybrid method and its applications. Fig. (5-a) shows the numerical results of the RCS analyses for open-ended cavities with a length of 100 mm, a high of 100 mm and a width of 100 mm. We combine IPO component with MPO component. This has been validated by comparison with MoM as the reference solution. MPO component make a small contribution to RCS from 0 degree to 90 degree, but make a large contribution to RCS from 90 degree to 180 degree. IPO component make a large contribution to RCS from 0 degree to 90 degree. The modified PO has higher accuracy than the original PO. Figs. (5-b) shows the numerical results of the RCS analyses for open-ended cavities with a length of 200 mm, a high of 200 mm and a width of 200 mm. This hybrid method shows a good agreement at all angles. Therefore, the results show validity as high frequency approximation.

5. Conclusion

We have developed a hybrid method in order to solve 3D problem having multiple reflections. The results of the hybrid method and the Moment Method coincide visibly. Therefore, we have shown validity of our hybrid method for high frequency approximation. We have shown application that we solve independently an inner problem and an outer problem.

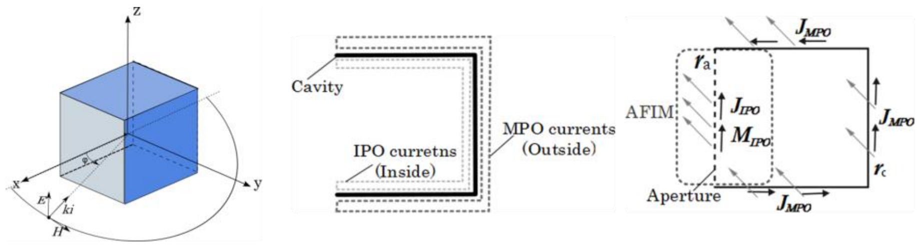

(1-a) (1-b) (1-C)

Fig. 1. Analysis model

(1-a)Scattering from open-ended cavities, (1-b) Currents distribution on the inner walls of the cavity and outer walls (1-C) radiation integral on the closed surface (Aperture and the external conducting wall)

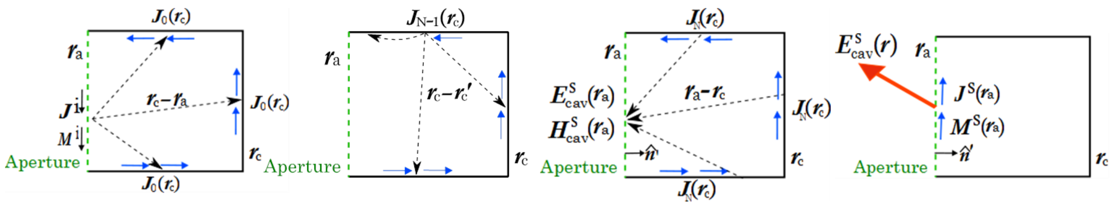

(2-a) (2-b) (2-c) (2-d)

Fig. 2. Iterative computation of currents on the inner walls and EM fields scattered by the cavity in the final step.

(2-a) Magnetic field induced on the inner walls of the cavity, (2-b) Iterative computation of currents induced on each facet of the inner walls of the cavity, (2-c) EM fields scattered by the cavity inner walls, (2-d) EM fields scattered at the observation point

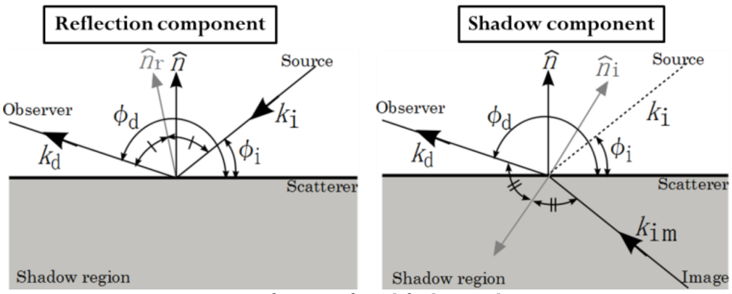

Fig. 3. Definition of modified normal vector

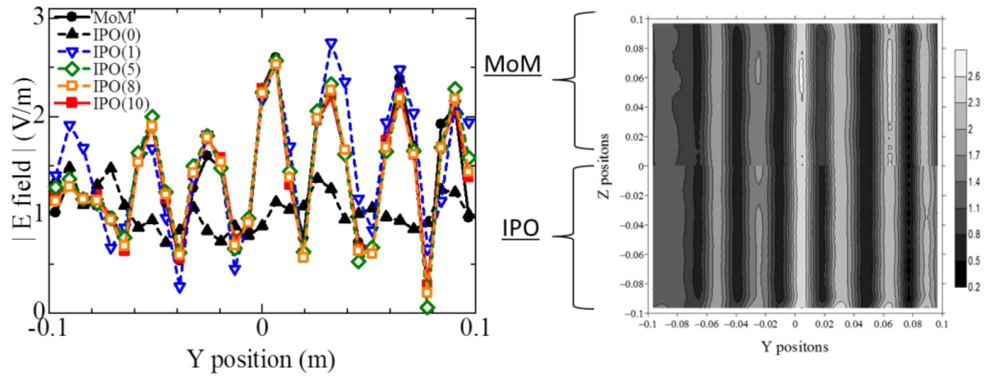

(4-a) (4-b)

Fig. 4. Electric field distribution of open-ended cavities, Frequency = 10 GHz, incident = 30 degree

(4-a) E field patterns of open-ended cavities at z positon = 0, (4-b) E field distribution of open-ended cavities on YZ plane

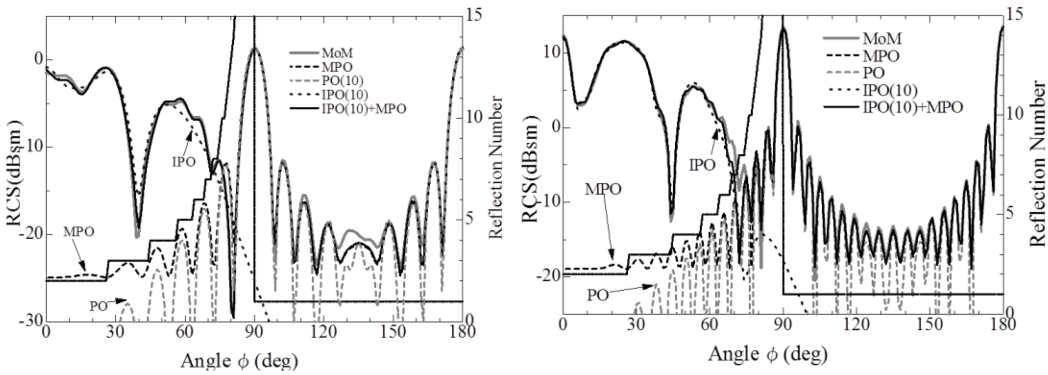

(5-a) (5-b)

Fig. 5. RCS patterns of open-ended cavities , Frequency = 10 GHz

(5-a) 100 mm open-ended cavities (5-b) 200 mm open-ended cavities

References

[1] Tetsu Shijo, Jun Goto, and Makoto Ando, "Modified Surface-normal Vector for improving Physical Optics," 2005 International Symposium on Antennas and Propagation (ISAP2005), TC3-4, Vol.2, pp.447-450, Seoul, KOREA, August 3-5, 2005.

[2] N. Omaki, T. Shijo and M. Ando, “PO with Modified Surface-normal Vectors for RCS calculation of Scatters with Edges and Wedges” IECIE Trans. Electron., vol.E85-A/B/C/D no.1, January, 2002.

[3] F.Obelleiro-Basterio and J.L.Rodriguez, “An Iterative Physical Optics Approach for Analyzing the Electromagnetic Scattering by Large Open-Ended Cavities,” IEEE Trans. Antenna Propagat. Vol.43, pp.356-361, Apr.1995

[4] R. Henmon, P. Pouliguen, H. He and J. Saillard and J. F. Damiens, “Computation of EM field Scattered by an Open-ended Cavity and by a cavity under Radome using the Iterative Physical Optics” IEEE Trans. Progress In Electromagnetic Research, PIER 80, 77-105, 208